

Superconductor-altermagnet memory functionality without stray fields

Hans Gløckner Giil¹ and Jacob Linder¹

¹Center for Quantum Spintronics, Department of Physics, Norwegian University of Science and Technology, NO-7491 Trondheim, Norway

A novel class of antiferromagnets, dubbed altermagnets, exhibit a non-relativistically spin-split band structure reminiscent of d -wave superconductors, despite the absence of net magnetization. This unique characteristic enables utilization in cryogenic stray-field-free memory devices, offering the possibility of achieving high storage densities. In this Letter, we determine how a proximate altermagnet influences the critical temperature T_c of a conventional s -wave singlet superconductor. Considering both a bilayer and trilayer, we show that such hybrid structures may serve as stray-field free memory devices where the critical temperature is controlled by rotating the Néel vector of one altermagnet, providing infinite magnetoresistance. Furthermore, our study reveals that altermagnetism can coexist with superconductivity up to a critical strength of the altermagnetic order as well as robustness of the altermagnetic influence on the conduction electrons against non-magnetic impurities, ensuring the persistence of the proximity effect under realistic experimental conditions.

Introduction— The intricate interplay of superconductivity and magnetism remains a focal point in modern condensed matter physics [1–3]. Its allure stems both from a fundamental viewpoint and cryogenic technology applications such as extremely sensitive detectors of radiation and heat as well as circuit components such as qubits and dissipationless diodes. Whereas superconductor-ferromagnet (SC-FM) structures have been studied extensively, the interest in antiferromagnetic materials has been comparatively limited [4–9] up until recently [10–19].

A particularly interesting new development is antiferromagnets that break time-reversal symmetry and feature a spin-split band structure that does not originate from relativistic effects such as spin-orbit coupling. Dubbed altermagnets in the literature, these are spin-compensated magnetic systems with a huge momentum-dependent spin splitting even in collinearly ordered antiferromagnets. *Ab initio* calculations have identified several possible material candidates that can host an altermagnetic state, including metals like RuO₂ and Mn₅Si₃ as well as semiconductors/insulators like MnF₂ and La₂CuO₄ [20–25].

Superconducting memory devices with infinite magnetoresistance have been proposed [26, 27] and observed [28] using superconducting spin-valves, a trilayer configuration comprised of a central superconductor flanked by two ferromagnets. By exploiting the inverse proximity effect, the critical temperature T_c of the superconductor can be dynamically modulated through manipulation of the relative magnetization orientations. In this way, T_c changes up to 1 K have been reported [29]. However, the property enabling the functionality of such structure via external fields is also its drawback, depending on the precise mode of operation: the magnetization. The disadvantage is the inevitable existence of a stray field surrounding the structure, which limits how closely multiple structures of this type can be packed together without disturbing each other. Therefore, finding a way to control T_c in a structure without any net magnetization could offer a major advantage to the implementation of such architecture in cryogenic devices. Recent strides in unraveling the altermagnet/superconductivity interplay encompass a spectrum of phenomena, including studies of Andreev reflection [30, 31], the Josephson effect [32–34], and interplay

with spin-orbit interaction [35].

In this Letter, we determine the effect of the altermagnetic spin splitting on the critical temperature of an adjacent superconductor and suggest using an AM-SC-AM trilayer as a stray field-free memory device. Commencing our study, we investigate a simple model demonstrating coexistence of altermagnetism and superconductivity and show that the altermagnetic field is detrimental to the superconducting order parameter, akin to the Pauli limit in superconductors subjected to magnetic fields [36]. Progressing to AM-SC bilayers, we unveil a modulation in the critical temperature, caused by the altermagnetic order. This modulation is non-monotonic as a function of the altermagnetic strength, and can both suppress or increase T_c compared to the normal metal case. We explore different geometries, showing that the relative direction of the interface and the altermagnetic order parameter yield vastly different results. A study of AM-SC-AM trilayers is then performed, highlighting the influence of the parallel or antiparallel directions of the order parameters in the two altermagnets. Finally, we investigate the role of impurities in the altermagnetic material. We find that impurities do not suppress the influence of altermagnetic spin order on the itinerant electrons, making the altermagnetic proximity effect relevant even in experiments utilizing materials that have a short mean free path.

Theory— The lattice Bogoliubov–de Gennes (BdG) framework [37, 38] is suitable for studying AM-SC heterostructures. We employ a mean-field Hamiltonian including altermagnetism and impurities,

$$\begin{aligned}
 H = E_0 - \sum_{i\sigma} (\mu - w_i) c_{i\sigma}^\dagger c_{i\sigma} - \sum_i (\Delta_i c_{i\downarrow}^\dagger c_{i\uparrow}^\dagger + \Delta_i^* c_{i\uparrow} c_{i\downarrow}) \\
 - \sum_{\langle i,j \rangle \sigma} t_{ij} c_{i\sigma}^\dagger c_{j\sigma} - \sum_{\langle i,j \rangle \sigma \sigma'} (\mathbf{m}_{ij} \cdot \boldsymbol{\sigma})_{\sigma \sigma'} c_{i\sigma}^\dagger c_{j\sigma'},
 \end{aligned} \tag{1}$$

where $c_{i\sigma}$ and $c_{i\sigma}^\dagger$ destroy and create an electron with spin σ , μ is the chemical potential, Δ_i the (site-dependent) superconducting order parameter, $\boldsymbol{\sigma} = (\sigma_1, \sigma_2, \sigma_3)$ is the Pauli vector, and w_i is an impurity potential taken to be randomly distributed at a given number of sites in the magnet. For comparison, we

consider two different forms of \mathbf{m}_{ij} : i) an on-site potential $\mathbf{m}_{ij} = m_z \delta_{ij} \hat{z}$, corresponding to a ferromagnetic term, and ii) $\mathbf{m}_{ij} = +m \mathbf{e}_z$ for nearest-neighbor hopping along the x axis and $\mathbf{m}_{ij} = -m \mathbf{e}_z$ for hopping along the y axis, corresponding to an effective altermagnetic term, similar to what was used in Ref. 32. The effect of the antiferromagnetic order in the localized spins exerted on the itinerant fermions $\{c_{i\sigma}, c_{i\sigma}^\dagger\}$ in the Hamiltonian Eq. (1) is thus modelled via \mathbf{m}_{ij} , owing to the fact that this is an effective model, where each site represents an average over a unit cell. We assume nearest neighbor hopping, i.e. $t_{ij} = t$, and scale all other parameters in units of t . The order parameter is determined from the site-dependent self-consistent gap equation,

$$\Delta_i = U_i \langle c_{i\uparrow} c_{i\downarrow} \rangle, \quad (2)$$

where U_i is the attractive potential. Throughout the paper, we fix $\mu = -t/2$ and $U_i = 1.7t$. The magnetic terms, superconducting order parameters, and impurity potentials are only nonzero in their respective regions. Specifically, the altermagnetic term \mathbf{m}_{ij} is finite only when both sites i, j inside are in the altermagnet.

Methodology— At each site i , the fermionic operators can be organized into Nambu vectors $\hat{c}_i \equiv (c_{i\uparrow}, c_{i\downarrow}, c_{i\uparrow}^\dagger, c_{i\downarrow}^\dagger)$, which may in turn be collected into a $4N$ -element vector $\check{c} \equiv (\hat{c}_1, \dots, \hat{c}_N)$ encompassing all fermionic lattice operators. The Hamiltonian operator is subsequently represented using a $4N \times 4N$ matrix: $H = E_0 + \frac{1}{2} \check{c}^\dagger \check{H} \check{c}$. We solve the BdG equation by numerically diagonalizing \check{H} and expressing physical observables such as the superconducting gap in Eq. (2) in terms of its eigenvectors and eigenvalues. This process entails an initial guess Δ_g for the order parameter, and then self-consistently diagonalizing the Hamiltonian until the superconducting gap equation converges. In this paper, however, our main interest is the critical temperature T_c , and thus we do not need the explicit numerical value of the gap. Instead, we perform N_Δ self-consistent iterations and compare the resulting value of the order parameter with the small initial value $\Delta_g = 10^{-4}t$. This solution strategy is very similar to the methodology used, e.g., in Ref. 39. We define the SC as being in the superconducting state when the median value of the order parameter inside the superconductor has increased compared to the initial value Δ_g . The critical temperature is subsequently ascertained by performing a binomial search in critical temperatures, as was done in Ref. 40.

Altermagnetic destruction of the superconducting order— Prior to delving into heterostructures of superconductors and altermagnets, it is instructive first to understand the effects of the altermagnetic term in Eq. (1) on the superconducting order. To this end, we consider a system with coexisting altermagnetic and superconducting order. We vary the altermagnetic strength m and calculate the critical temperature self-consistently using the methodology outlined above. The results are shown in Fig. 1: the effect of altermagnetism is to suppress the superconducting order, which vanishes for an altermagnetic strength of $m \approx 0.05t$. The results are juxtaposed with the effects of

ferromagnetism, which also suppresses the superconductivity in a similar way, as is well-known [36, 41], although the critical field is much larger than in the altermagnetic case.

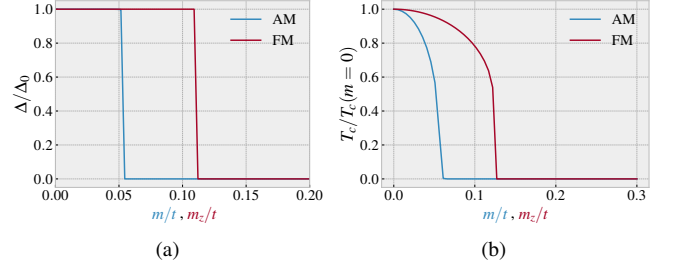


FIG. 1. The (a) order parameter and (b) critical temperature as a function of the alter- and ferromagnetic strength in a $N_x = N_y = 20a_0$ structure with coexisting superconductivity and altermagnetic/ferromagnetic spin splitting.

After establishing the analogous interaction between the altermagnetic and ferromagnetic terms with superconductivity, a natural inquiry arises regarding the impact of altermagnets on superconductors within heterostructures. Specifically, we shall focus our attention on the influence of altermagnets on the critical temperature within AM-SC systems.

Junction geometries— Employing a square lattice with lattice constant a_0 , we explore two distinct AM-SC geometries: a straight junction, where the interface is aligned with the crystallographic axis, and a skewed junction, where the interface is rotated 45° compared with the crystallographic axis, see Fig. 2. We denote the number of lattice sites in the x (y) direction by $N_{x(y)}$. In the straight junction, hopping across the interface happens exclusively along the x -axis, while in the skewed junction, hopping across the interface happens equally along the x - and y - axis. The inverse proximity effect in the SC-AM system

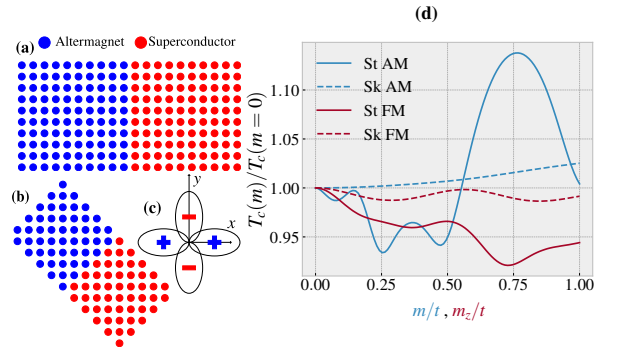


FIG. 2. The (a) straight junction and (b) the skewed junction geometries. (c) the hopping term for a spin-up (spin-down) electron (hole). For a spin-down (spin-up) electron (hole), the signs are reversed. In (d): the critical temperature for the straight (St) and skewed (Sk) geometries with $N_y = 20a_0$, $N_x^{AM} = 10a_0$, $N_x^{SC} = 6a_0$, and $N_\Delta = 50$.

can be probed by calculating the critical temperature T_c in the SC. The result is depicted in Fig. 2, highlighting a significant

disparity in the behavior between the straight and skewed junction configurations. In the skewed junction, the effect of the altermagnetism is to suppress Andreev reflection [42], which is the underlying mechanism causing the (inverse) proximity effect. This happens because the altermagnetic term causes different hopping for electrons and holes involved in Andreev reflection. Thus, the inverse proximity effect is suppressed for high values of m , causing the critical temperature to increase. In the case of the straight junction, an additional factor comes into play—induced magnetization brought about by the inverse proximity effect [43]. This phenomenon leads to a pronounced oscillatory behavior in the critical temperature. The induced magnetization can be understood by noting that spin-up electrons favor hopping in the x -direction, causing leaking spin-up electrons from the SC into the AM to be trapped in the AM for large m . In the skewed junction, this effect is averaged out, and the induced magnetization in the SC vanishes.

AM-SC-AM trilayers— An intriguing extension to the discussion above can be achieved by adding another altermagnet to the AM-SC system considered above. This system entails two distinct scenarios: one where the two altermagnets are aligned and one where the second altermagnet is rotated (in real space) by 90° . We refer to these situations as a parallel (P) and antiparallel (AP) alignment, see Fig. 3. Rotating the second altermagnet is akin to changing the sign of m in this region, or equivalently to a 180° rotation in spin space. In Fig. 3b, the critical temperature of the SC is calculated for different values of m in the two different systems. In the P alignment, the situation is analogous to the AM-SC system considered above, and we see a similar T_c modulation pattern. In the AP alignment case, the critical temperature is lower than in the P alignment for most values of m . To understand why this is the case, we note that the superconducting coherence length in our system $\xi_S = \hbar v_F / \pi \Delta_0$ is comparable to the system length, as is often the regime investigated experimentally. In light of this, we attribute the lower critical temperature to the appearance of crossed Andreev reflection (CAR), sometimes referred to as nonlocal Andreev reflection [44]. It is well known that for an F-S-F heterostructure, the AP alignment of ferromagnets gives enhanced CAR compared to the AP alignment [45], and we attribute the results of Fig. 3b to a similar origin. Importantly, switching between the P and AP alignment can experimentally be performed by rotating the Néel vector, since this effectively switches the spin-up and spin-down bands in the altermagnet. A similar T_c modulation in conventional antiferromagnets was very recently reported [46]. Notably, the Néel vector has been found to be controllable by spin transfer torques [47, 48], spin-orbit torques [49], and by optical methods [50]. This opens the possibility of using the suggested device as a stray field-free memory device operating in the THz regime, enabling the prospect of ultrafast switching.

Impurity scattering— Materials with substantial impurity scattering are highly relevant for experiments. For this reason, we will concentrate on the role of impurities in altermagnets, before moving on to the proximity effect in a system with a dirty altermagnet. Impurities are accounted for through an

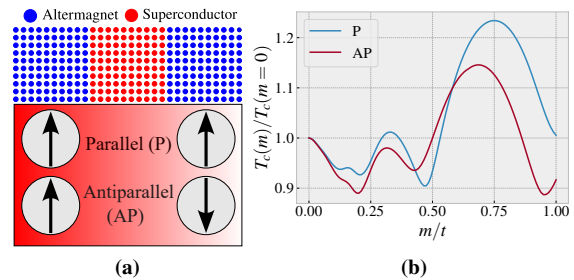


FIG. 3. In (a): the AM-SC-AM system with P and AP alignment of the altermagnets. In (b): the critical temperatures in a system where the length of the SC is $12a_0$, and $N_y = 20a_0$. The altermagnets on either side have a length of $10a_0$.

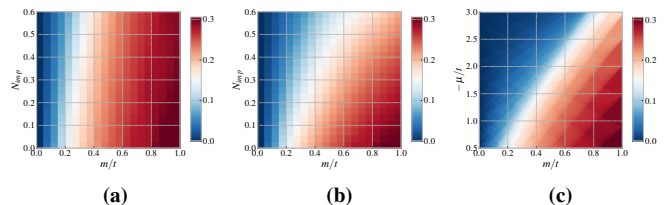


FIG. 4. ΔC_\uparrow as a function of m and N_i , for impurity strength of (a): $w_i = 1t$ and (b) $w_i = 3t$. In (c): ΔC_\uparrow as a function of m and μ in a system without impurities. The system size is $N_x = N_y = 20a_0$.

on-site potential [51–53] at a fraction N_i of all sites, with a fixed strength w_i , and randomly chosen sites in the altermagnet, similar to the methodology in Ref. 53. Observables are calculated by averaging over 100 different impurity configurations. As the impurity scattering is isotropic, one might expect that the altermagnetic spin-splitting, which is anisotropic, disappears in the presence of impurities. To test this, we define the *bona fide* order parameter ΔC_\uparrow ,

$$\Delta C_\uparrow = \sum_i \left[\langle c_{i\uparrow}^\dagger c_{i+\hat{x}\uparrow} \rangle - \langle c_{i\uparrow}^\dagger c_{i+\hat{y}\uparrow} \rangle \right], \quad (3)$$

which is a measure of the anisotropy of the effective hopping parameter (for spin-up particles) in the system, and depends on both t and m in general. For square systems, we expect the system to be invariant under C_4 rotations for $m = 0$, i.e. $\Delta C_\uparrow = 0$. Thus, we can use ΔC_\uparrow to determine whether the system is altermagnetic or not. In Fig. 4, we plot the results for different values of m and N_i , for $w_i = 1.0t$ and $w_i = 3.0t$, comparable to other values used in the literature [52]. Evidently, the altermagnetic order is resilient to the non-magnetic impurities in the system; the slight suppression of the order parameter for strong impurity scattering (i.e. the upper parts of the plots in Fig. 4b) can be explained by an effective renormalized chemical potential as in Fig. 4c. Finally, we repeat the calculations of the skewed junction in Fig. 2, including impurities in the AM. We set the strength of the impurities to $w_i = 1.0t$ and the fraction of sites occupied by impurities to 0.2, and perform the calculations for 100 different impurity

configurations, before averaging over the resulting values of the critical temperature. The results are shown in Fig. 5, and show that although the critical temperature curve is different from the clean system, the (inverse) proximity effect is still present, which is evident from the fact that the critical temperature varies with a similar magnitude compared with the clean system. The slight increase in T_c in the presence of impurities, indicating a suppressed superconducting proximity effect, is consistent with the recent findings of Ref. [17]. Thus, we conclude that impurities are not strongly detrimental to the altermagnetic modulation of the superconducting order, which means that the effect should be experimentally visible even for dirty materials. We have thus found that the analogy between d -wave superconductor and altermagnetism [25] is not useful in impurity considerations: whereas d -wave superconductivity is highly sensitive to non-magnetic impurities, the altermagnetic effect on the conduction electrons survives even in the presence strong impurity potentials. This is due to the “ d -wave” Fermi surface of altermagnets being spin-split, prohibiting the scattering between the spin bands in the absence of spin-flip impurities.

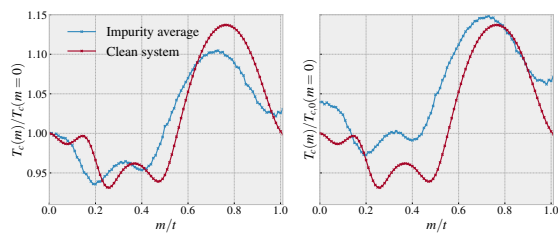


FIG. 5. The impurity average plotted together with the clean system, which is the same as the straight system in Fig. 2b. In the right pane, the temperatures are normalized to the zero-impurity and zero-magnetism critical temperature $T_{c,0}(m=0)$, showing that T_c is slightly higher in the presence of impurities. In the left pane, the temperatures are normalized to unity for $m=0$, i.e. the two curves are normalized differently, which illustrates that the variation in T_c with m is of similar magnitude in both cases.

Conclusion— We have solved the lattice Bogoliubov-de Gennes equations in heterostructures of superconductors and altermagnets. Our study indicates that altermagnetic materials have the potential to be used in cryogenic spintronic devices, for instance as stray-field-free spin switches showing infinite magnetoresistivity, using spin-transfer torques, spin-orbit torques, or optical methods to rotate the Néel vector. Non-magnetic impurities are not severely detrimental to the altermagnetic proximity effect, allowing for this effect to be present also in altermagnetic materials in the diffusive transport regime.

We thank J. A. Ouassou, E. W. Hodt, and B. Brekke for helpful comments and discussions. This work was supported by the Research Council of Norway through Grant No. 323766 and its Centres of Excellence funding scheme Grant No. 262633 “QuSpin.” Support from Sigma2 - the National Infrastructure for High Performance Computing and Data Storage in Norway, project NN9577K, is acknowledged.

- [1] F. S. Bergeret, A. F. Volkov, and K. B. Efetov, *Rev. Mod. Phys.* **77**, 1321 (2005).
- [2] A. I. Buzdin, *Rev. Mod. Phys.* **77**, 935 (2005).
- [3] F. S. Bergeret, M. Silaev, P. Virtanen, and T. T. Heikkilä, *Rev. Mod. Phys.* **90**, 041001 (2018).
- [4] B. M. Andersen, I. V. Bobkova, P. J. Hirschfeld, and Y. S. Barash, *Phys. Rev. Lett.* **96**, 117005 (2006).
- [5] B. M. Andersen, I. V. Bobkova, P. J. Hirschfeld, and Y. S. Barash, *Phys. Rev. B* **72**, 184510 (2005).
- [6] C. Bell, E. J. Tarte, G. Burnell, C. W. Leung, D.-J. Kang, and M. G. Blamire, *Phys. Rev. B* **68**, 144517 (2003).
- [7] M. Hübener, D. Tikhonov, I. A. Garifullin, K. Westerholt, and H. Zabel, *J. Phys.: Condens. Matter* **14**, 8687 (2002).
- [8] B. L. Wu, Y. M. Yang, Z. B. Guo, Y. H. Wu, and J. J. Qiu, *Appl. Phys. Lett.* **103**, 152602 (2013).
- [9] H. Enoksen, J. Linder, and A. Sudbø, *Phys. Rev. B* **88**, 214512 (2013).
- [10] L. G. Johnsen, S. H. Jacobsen, and J. Linder, *Phys. Rev. B* **103**, L060505 (2021).
- [11] G. A. Bobkov, I. V. Bobkova, A. M. Bobkov, and A. Kamra, *Phys. Rev. B* **106**, 144512 (2022).
- [12] D. S. Rabinovich, I. V. Bobkova, and A. M. Bobkov, *Phys. Rev. Res.* **1**, 033095 (2019).
- [13] V. Falch and J. Linder, *Phys. Rev. B* **106**, 214511 (2022).
- [14] M. F. Jakobsen, K. B. Naess, P. Dutta, A. Brataas, and A. Qaiumzadeh, *Phys. Rev. B* **102**, 140504 (2020).
- [15] J. L. Lado and M. Sigrist, *Phys. Rev. Lett.* **121**, 037002 (2018).
- [16] E. H. Fyhn, A. Brataas, A. Qaiumzadeh, and J. Linder, *Phys. Rev. B* **107**, 174503 (2023).
- [17] E. H. Fyhn, A. Brataas, A. Qaiumzadeh, and J. Linder, *Phys. Rev. Lett.* **131**, 076001 (2023).
- [18] G. A. Bobkov, I. V. Bobkova, and A. M. Bobkov, *Phys. Rev. B* **108**, 054510 (2023).
- [19] S. Chourasia, L. J. Kamra, I. V. Bobkova, and A. Kamra, arXiv:2303.18145 (2023).
- [20] S. Hayami, Y. Yanagi, and H. Kusunose, *J. Phys. Soc. Jpn.* **88**, 123702 (2019).
- [21] K.-H. Ahn, A. Hariki, K.-W. Lee, and J. Kunes, *Phys. Rev. B* **99**, 184432 (2019).
- [22] S. López-Moreno, A. H. Romero, J. Mejía-López, and A. Muñoz, *Phys. Chem. Chem. Phys.* **18**, 33250 (2016), publisher: The Royal Society of Chemistry.
- [23] L. Šmejkal, R. González-Hernández, T. Jungwirth, and J. Sinova, *Sci. Adv.* **6**, eaaz8809 (2020).
- [24] H. Reichlová, R. L. Seeger, R. González-Hernández, I. Kounta, R. Schlitz, D. Kriegner, P. Ritzinger, M. Lammel, M. Leiviskä, V. Petříček, P. Doležal, E. Schmoranzarová, A. Bad’ura, A. Thomas, V. Baltz, L. Michez, J. Sinova, S. T. B. Goennenwein, T. Jungwirth, and L. Šmejkal, Macroscopic time reversal symmetry breaking by staggered spin-momentum interaction (2021), arxiv:2012.15651 [cond-mat].
- [25] L. Šmejkal, J. Sinova, and T. Jungwirth, *Phys. Rev. X* **12**, 031042 (2022).
- [26] A. I. Buzdin, A. V. Vedyayev, and N. V. Ryzhanova, *Europhys. Lett.* **48**, 686 (1999).
- [27] L. R. Tagirov, *Phys. Rev. Lett.* **83**, 2058 (1999).
- [28] B. Li, N. Roschewsky, B. A. Assaf, M. Eich, M. Epstein-Martin, D. Heiman, M. Münzenberg, and J. S. Moodera, *Phys. Rev. Lett.* **110**, 097001 (2013).
- [29] A. Singh, S. Voltan, K. Lahabi, and J. Aarts, *Phys. Rev. X* **5**, 021019 (2015).

- [30] C. Sun, A. Brataas, and J. Linder, *Phys. Rev. B* **108**, 054511 (2023).
- [31] M. Papaj, Andreev reflection at altermagnet/superconductor interface (2023), [arxiv:2305.03856](https://arxiv.org/abs/2305.03856) [cond-mat].
- [32] J. A. Ouassou, A. Brataas, and J. Linder, *Phys. Rev. Lett.* **131**, 076003 (2023).
- [33] S.-B. Zhang, L.-H. Hu, and T. Neupert, Finite-momentum Cooper pairing in proximitized altermagnets (2023), [arxiv:2302.13185](https://arxiv.org/abs/2302.13185) [cond-mat].
- [34] C. W. J. Beenakker and T. Vaktel, Phase-shifted Andreev levels in an altermagnet Josephson junction (2023), [arxiv:2306.16300](https://arxiv.org/abs/2306.16300) [cond-mat].
- [35] M. Wei, L. Xiang, F. Xu, L. Zhang, G. Tang, and J. Wang, Gapless superconducting state and mirage gap in altermagnets (2023), [arxiv:2308.00248](https://arxiv.org/abs/2308.00248) [cond-mat].
- [36] A. M. Clogston, *Phys. Rev. Lett.* **9**, 266 (1962).
- [37] J.-X. Zhu, *Bogoliubov-de Gennes Method and Its Applications*, Lecture Notes in Physics, Vol. 924 (Springer International Publishing, Cham, 2016).
- [38] P. G. de Gennes, *Superconductivity of metals and alloys* (W.A. Benjamin, 1966).
- [39] L. G. Johnsen, K. Svalland, and J. Linder, *Phys. Rev. Lett.* **125**, 107002 (2020).
- [40] J. A. Ouassou, *Manipulating Superconductivity in Magnetic Nanostructures in and out of Equilibrium*, Ph.D. thesis, Norwegian University of Science and Technology, Trondheim (2019).
- [41] B. S. Chandrasekhar, *Appl. Phys. Lett.* **1**, 7 (1962).
- [42] A. F. Andreev, *Sov. Phys. JETP*. **19** (1964).
- [43] J. Linder and J. W. A. Robinson, *Nature Phys* **11**, 307 (2015).
- [44] G. Falci, D. Feinberg, and F. W. J. Hekking, *Europhys. Lett.* **54**, 255 (2001).
- [45] G. Deutscher and D. Feinberg, *Appl. Phys. Lett.* **76**, 487 (2000).
- [46] L. J. Kamra, S. Chourasia, G. A. Bobkov, V. M. Gordeeva, I. V. Bobkova, and A. Kamra, Infinite magnetoresistance and N\`eel triplets-mediated exchange in antiferromagnet-superconductor-antiferromagnet trilayers (2023), [arxiv:2306.11373](https://arxiv.org/abs/2306.11373) [cond-mat].
- [47] R. Cheng, M. W. Daniels, J.-G. Zhu, and D. Xiao, *Phys. Rev. B* **91**, 064423 (2015).
- [48] S. Urazhdin and N. Anthony, *Phys. Rev. Lett.* **99**, 046602 (2007).
- [49] Z. Xu, J. Ren, Z. Yuan, Y. Xin, X. Zhang, S. Shi, Y. Yang, and Z. Zhu, *J. Appl. Phys.* **133**, 153904 (2023).
- [50] V. Grigorev, M. Filianina, Y. Lytvynenko, S. Sobolev, A. R. Pokharel, A. P. Lanz, A. Sapozhnik, A. Kleibert, S. Bodnar, P. Grigorev, Y. Skourski, M. Kläui, H.-J. Elmers, M. Jourdan, and J. Demsar, *ACS Nano* **16**, 20589 (2022).
- [51] Y. Asano, Y. Sawa, Y. Tanaka, and A. A. Golubov, *Phys. Rev. B* **76**, 224525 (2007).
- [52] Y. Asano, Y. Tanaka, and A. A. Golubov, *Phys. Rev. Lett.* **98**, 107002 (2007).
- [53] Z.-X. Li, S. A. Kivelson, and D.-H. Lee, *npj Quantum Mater.* **6**, 36 (2021).